Synthesis and Luminescence Behavior of Rhenium(I) Triynyl Complexes. X-ray Crystal Structures of $[Re(CO)_3(^tBu_2bpy)(C{\equiv}C{-}C{\equiv}C{-}C{\equiv}CPh)]$ and $[Re(CO)_3(Me_2bpy)(C{\equiv}C{-}C{\equiv}C{-}C{\equiv}CSiMe_3)]$

Vivian Wing-Wah Yam,* Samuel Hung-Fai Chong, Chi-Chiu Ko, and Kung-Kai Cheung

Department of Chemistry, The University of Hong Kong, Pokfulam Road, Hong Kong, People's Republic of China

Received August 21, 2000

Luminescent rhenium(I) triynyl complexes $[Re(CO)_3(^tBu_2bpy)(C{\equiv}C{-}C{\equiv}C{-}C{\equiv}CPh)]$ **1**, $[Re(CO)_3(^tBu_2bpy)(C{\equiv}C{-}C{\equiv}C{-}C{\equiv}CSiMe_3)]$ **2**, and $[Re(CO)_3(Me_2bpy)(C{\equiv}C{-}C{\equiv}C{-}C{\equiv}CSiMe_3)]$ **3**, were synthesized and their photophysical and electrochemical properties studied. The X-ray crystal structures of **1** and **3** have also been determined. A comparison study of their emission properties to that of their mono- and diynyl analogues was made and their emission origin suggested and supported by EHMO studies.

Introduction

There has been a rapidly growing interest in the unique chemical and physical properties of C_n-bridged metal-containing materials,[1] especially those with long sp carbon chains, in view of their potential applications as nonlinear optical materials, molecular wires, and molecular electronics. Organic polyynes are known to show emissive behavior,[2] most of which are fluorescent in nature. It is envisaged that incorporation of heavy metal centers into the polyyne system may render it phosphorescent and increase the lifetime of photoluminescence, as a result of a larger spin−orbit coupling. Despite a number of works on the luminescence behavior of the metal-containing monoyne and diyne complexes,[3] to the best of our knowledge, luminescence studies of the polyyne counterparts are rare.[4] With the recent reports on the successful isolation of acetylide-bridged rhenium(I) organometallics[5] and our recent efforts in incorporating metal-to-ligand charge transfer (MLCT) excited states into rhenium(I) acetylide units to make luminescent rigid-rod materials,[3a,b,f] we have extended our work to systematically elongate the carbon chain from a diynyl to triynyl unit. Herein are reported the synthesis, structure, and luminescence behavior of three rhenium(I) triynyl complexes, $[Re(CO)_3(^tBu_2bpy)(C{\equiv}C{-}C{\equiv}C{-}C{\equiv}CPh)]$ (**1**), $[Re(CO)_3(^tBu_2bpy)(C{\equiv}C{-}C{\equiv}C{-}C{\equiv}CSiMe_3)]$ (**2**), and $[Re(CO)_3(Me_2bpy)(C{\equiv}C{-}C{\equiv}C{-}C{\equiv}CSiMe_3)]$ (**3**).

Experimental Section

Materials and Reagents. $[Re(CO)_5Cl]$ was obtained from Strem Chemicals, Inc. 4,4′-Dimethyl-2,2′-bipyridine (Me_2bpy) was obtained from Aldrich Chemical Co. 4,4′-Di-*tert*-butyl-2,2′-bipyridine ($^tBu_2bpy$) was prepared by the slight modification of a reported procedure.[6] $[Re(CO)_3(^tBu_2bpy)(C{\equiv}C{-}C{\equiv}CH)]$ and $[Re(CO)_3(Me_2bpy)(C{\equiv}C{-}C{\equiv}CH)]$ were synthesized as previously described.[3f] 1-Iodo-2-(trimethylsilyl)acetylene, copper(I) iodide, and piperidine were purchased from Aldrich Chemical Co. 1-Bromo-2-(phenyl)acetylene was prepared by the slight modification of a reported procedure.[7] All solvents

* Corresponding author. Tel: (852)2859−2153. Fax: (852)2857-1586. E-mail: wwyam@hku.hk.

(1) (a) Manna, J.; John, K. D.; Hopkins, M. D. *Adv. Organomet. Chem*. **1995**, *38*, 79. (b) Touchard, D.; Haquette, P.; Guesmi, S.; Pichon, L. L.; Daridor, A.; Toupet, L.; Dixneuf, P. H. *Organometallics* **1997**, *16*, 3640. (c) Weyland, T.; Lapinte, C.; Frapper, G.; Calhorda, M. J.; Halet, J. F.; Toupet, L. *Organometallics* **1997**, *16*, 2024. (d) Lewis, J.; Long, N. J.; Raithby, P. R.; Shields, G. P.; Wong, W. Y.; Younus, M. *J. Chem. Soc., Dalton Trans.* **1997**, 4283. (e) Hartbaum, C.; Fischer, H. *Chem. Ber*. **1997**, *130*, 1063. (f) Bruce, M. I. *Coord. Chem. Rev*. **1997**, *166*, 91. (g) Ziessel, R.; Hissler, M.; El-ghayoury, A.; Harriman, A. *Coord. Chem. Rev*. **1998**, *178−180*, 1251. (h) Bruce, M. I.; Ke, M.; Low, P. J.; Skelton, B. W.; White, A. H. *Organometallics* **1998**, *17*, 3539. (i) Bruce, M. I.; Skelton, B. W.; White, A. H.; Zaitseva, N. N. *J. Organomet. Chem*. **1998**, *558*, 197. (j) Roth, G.; Fischer, H. *Organometallics* **1998**, *17*, 1511. (k) Cadierno, V.; Gamasa, M. P.; Gimeno, J. *Organometallics* **1998**, *17*, 697. (l) Morton, M. S.; Selegue, J. P. *J. Organomet. Chem*. **1999**, *578*, 133. (m) Roidl, G.; Enkelmann, V.; Adams, R. D.; Bunz, U. H. F. *J. Organomet. Chem*. **1999**, *578*, 144. (n) Coat, F.; Guillemot, M.; Paul, F.; Lapinte, C. *J. Organomet. Chem*. **1999**, *578*, 76. (o) Stang, S. L.; Lenz, D.; Paul, F.; Lapinte, C. *J. Organomet. Chem*. **1999**, *572*, 189.

(2) See for example: Devadoss, C.; Bharathi, P.; Moore, J. S. *J. Am. Chem. Soc*. **1996**, *118*, 9635.

(3) (a) Yam, V. W. W.; Lau, V. C. Y.; Cheung, K. K. *Organometallics* **1995**, *14*, 2749. (b) Yam, V. W. W.; Lau, V. C. Y.; Cheung, K. K. *Organometallics* **1996**, *15*, 1740. (c) Yam, V. W. W.; Choi, S. W. K.; Cheung, K. K. *Organometallics* **1996**, *15*, 1734. (d) Yam, V. W. W.; Fung, W. K. M.; Cheung, K. K. *Chem. Commun*. **1997**, 963. (e) Yam, V. W. W.; Fung, W. K. M.; Wong, K. M. C.; Lau, V. C. Y.; Cheung, K. K. *Chem. Commun*. **1998**, 777. (f) Yam, V. W. W.; Chong, S. H. F.; Cheung, K. K. *Chem. Commun*. **1998**, 2121. (g) Yam, V. W. W.; Chong, S. H. F.; Wong, K. M. C.; Cheung, K. K. *Chem. Commun*. **1999**, 1013. (h) Yam, V. W. W.; Lo, K. K. W.; Wong, K. M. C. *J. Organomet. Chem*. **1999**, *578*, 3.

(4) Hartbaum, J.; Fischer, H. *J. Organomet. Chem*. **1999**, *578*, 186.

(5) (a) Heidrich, J.; Steimann, M.; Appel, M.; Beck, W. *Organometallics* **1990**, *9*, 1296. (b) Weng, W.; Bartik, T.; Brady, M.; Bartik, B.; Ramsden, J. A.; Arif, A. M.; Gladysz, J. A. *J. Am. Chem. Soc*. **1995**, *117*, 11922. (c) Bunz, U. H. F. *Angew. Chem., Int. Ed. Engl*. **1996**, *35*, 969. (d) Brady, M.; Weng, W.; Zhou, Y.; Seyler, J. W.; Amoroso, A. J.; Arif, A. M.; Bohme, M.; Frenking, G.; Gladysz, J. A. *J. Am. Chem. Soc*. **1997**, *119*, 775. (e) Falloon, S. B.; Weng, W.; Arif, A. M.; Gladysz, J. A. *Organometallics* **1997**, *16*, 2008. (f) Bartik, T.; Weng, W.; Ramsden, J. A.; Szafert, S.; Falloon, S. B.; Arif, A. M.; Gladysz, J. A. *J. Am. Chem. Soc*. **1998**, *120*, 11071. (g) Belanzoni, P.; Re, N.; Sgamellotti, A.; Floriani, C. *J. Chem. Soc., Dalton Trans*. **1998**, 1825. (h) Falloon, S. B.; Szafert, S.; Arif, A. M.; Gladysz, J. A. *Chem. Eur. J*. **1998**, *4*, 1033. (i) Dembinski, R.; Lis, T.; Szafert, S.; Mayne, C. L.; Bartik, T.; Gladysz, J. A. *J. Organomet. Chem*. **1999**, *578*, 229.

(6) Hadda, T. B.; Bozec, H. L. *Polyhedron* **1988**, *7*, 75.

10.1021/om000725b CCC: $19.00
Publication on Web 10/28/2000

were purified and distilled using standard procedures before use.[8] All other reagents were of analytical grade and were used as received.

Syntheses of Rhenium Complexes. All reactions were performed under anaerobic and anhydrous conditions using standard Schlenk techniques under an inert atmosphere of nitrogen.

[Re(CO)$_3$(^{t}Bu$_2$bpy)(C≡C−C≡C−C≡CPh)] (1). A mixture of [Re(CO)$_3$(^{t}Bu$_2$bpy)(C≡C−C≡CH)] (100 mg, 0.17 mmol), BrC≡CPh (0.17 mmol), piperidine (0.67 mL, 6.80 mmol), and CuI (0.0051 mmol) in THF (40 mL) was stirred at room temperature in an inert atmosphere of nitrogen for 15 min, after which the solvent was removed under vacuum. The product was then purified by column chromatography on silica gel using dichloromethane−petroleum ether (1:1 v/v) as eluent. Subsequent recrystallization from dichloromethane−*n*-hexane gave orange crystals of **1** (yield 41 mg, 35%). ^{1}H NMR (300 MHz, acetone-d_6, 298 K, relative to Me$_4$Si): δ 1.40 (s, 18H, ^{t}Bu), 7.30 (m, 5H, Ph H's), 7.70 (dd, 2H, J = 1.7 and 5.9 Hz, 5- and 5'-pyridyl H's), 8.70 (d, 2H, J = 1.7 Hz, 3- and 3'-pyridyl H's), 8.90 (d, 2H, J = 5.9 Hz, 6- and 6'-pyridyl H's). IR (Nujol mull, ν/cm^{-1}): 2155, 2131, 2030, 2002, 1926, 1889 ν(C≡O, C≡C). Positive FAB-MS: ion clusters at m/z 688 {M}$^+$, 660 {M − CO}$^+$, 539 {M − [C≡C−C≡C−C≡CPh]}$^+$. Anal. Found: C 57.58, H 4.56, N 3.84. Calcd for **1**: C 57.64, H 4.22, N 4.08.

[Re(CO)$_3$(^{t}Bu$_2$bpy)(C≡C−C≡C−C≡CSiMe$_3$)] (2). A mixture of [Re(CO)$_3$(^{t}Bu$_2$bpy)(C≡C−C≡CH)] (100 mg, 0.17 mmol), IC≡CSiMe$_3$ (0.17 mmol), piperidine (0.67 mL, 6.80 mmol), and CuI (0.0051 mmol) in THF (40 mL) was stirred at room temperature in an inert atmosphere of nitrogen for 15 min, after which the solvent was removed under vacuum. The product was then purified by column chromatography on silica gel using dichloromethane−petroleum ether (4:1 v/v) as eluent. Subsequent recrystallization from dichloromethane−*n*-hexane gave orange crystals of **2** (yield 47 mg, 40%). ^{1}H NMR (300 MHz, acetone-d_6, 298 K, relative to Me$_4$Si): δ 0.10 (s, 9H, Me$_3$Si−), 1.50 (s, 18H, ^{t}Bu), 7.80 (dd, 2H, J = 1.8 and 5.9 Hz, 5- and 5'-pyridyl H's), 8.70 (d, 2H, J = 1.8 Hz, 3- and 3'-pyridyl H's), 8.90 (d, 2H, J = 5.9 Hz, 6- and 6'-pyridyl H's). IR (Nujol mull, ν/cm^{-1}): 2151, 2095, 2017, 1994, 1934, 1889 ν(C≡O, C≡C). Positive FAB-MS: ion clusters at m/z 656 {M − CO}$^+$, 539 {M − [C≡C−C≡C−C≡CSiMe$_3$]}$^+$. Anal. Found: C 54.16, H 5.36, N 3.58. Calcd for **2**·1/2THF: C 54.03, H 5.43, N 3.71.

[Re(CO)$_3$(Me$_2$bpy)(C≡C−C≡C−C≡CSiMe$_3$)] (3). The procedure is similar to that described for the preparation of **2**, except [Re(CO)$_3$(Me$_2$bpy)(C≡C−C≡CH)] was used in place of [Re(CO)$_3$(^{t}Bu$_2$bpy)(C≡C−C≡CH)] to give orange crystals of **3** (yield 42 mg, 35%). ^{1}H NMR (300 MHz, acetone-d_6, 298 K, relative to Me$_4$Si): δ 0.10 (s, 9H, Me$_3$Si−), 2.60 (s, 6H, methyl H's on Me$_2$-bpy), 7.60 (dd, 2H, J = 1.8 and 5.7 Hz, 5- and 5'-pyridyl H's), 8.60 (d, 2H, J = 1.8 Hz, 3- and 3'-pyridyl H's), 8.90 (d, 2H, J = 5.7 Hz, 6- and 6'-pyridyl H's). IR (Nujol mull, ν/cm^{-1}): 2129, 2023, 2005, 1964, 1939, 1897 ν(C≡O, C≡C). Positive FAB-MS: ion clusters at m/z 601 {M}$^+$, 572 {M − CO}$^+$, 455 {M − [C≡C−C≡C−C≡CSiMe$_3$]}$^+$. Anal. Found: C 48.71, H 3.53, N 4.58. Calcd for **3**·1/2THF: C 49.10, H 3.93, N 4.40.

Physical Measurements and Instrumentation. UV−visible spectra were obtained on a Hewlett-Packard 8452A diode array spectrophotometer, IR spectra as Nujol mulls on a Bio-Rad FTS-7 Fourier transform infrared spectrophotometer (4000−400 cm^{-1}), and steady-state excitation and emission spectra on a Spex Fluorolog 111 spectrofluorometer equipped with a Hamamatsu R-928 photomultiplier tube. Low-temperature (77 K) spectra were recorded by using an optical Dewar sample holder. ^{1}H NMR spectra were recorded on a Bruker DPX-300 (300 MHz) Fourier transform NMR spectrometer with chemical shifts recorded relative to Me$_4$Si. Positive ion FAB mass spectra were recorded on a Finnigan MAT95 mass spectrometer. Elemental analyses of the new complexes were performed on a Carlo Erba 1106 elemental analyzer at the Institute of Chemistry, Chinese Academy of Sciences.

Emission-lifetime measurements were performed using a conventional laser system. The excitation source was the 355 nm output (third harmonic) of a Quanta-Ray Q-switched GCR-150 pulsed Nd:YAG laser (10 Hz). Luminescence decay signals were recorded on a Tektronix Model TDS-620A (500 MHz, 2 GS/s) digital oscilloscope and analyzed using a program for exponential fits. All solutions for photophysical studies were degassed on a high-vacuum line in a two-compartment cell consisting of a 10 mL Pyrex bulb and a 1 cm path length quartz cuvette and sealed from the atmosphere by a Bibby Rotaflo HP6 Teflon stopper. The solutions were subject to at least four freeze−pump−thaw cycles.

Cyclic voltammetric measurements were performed by using a CH Instruments, Inc. Model CHI 620 electrochemical analyzer interfaced to an IBM-compatible personal computer. The electrolytic cell used was a conventional two-compartment cell. The salt bridge of the reference electrode was separated from the working electrode compartment by a Vycor glass. A Ag/AgNO$_3$ (0.1 M in CH$_3$CN) reference electrode was used. The ferrocenium−ferrocene couple was used as the internal standard in the electrochemical measurements in acetonitrile (0.1 M ^{n}Bu$_4$NPF$_6$).[9a] The working electrode was a glassy-carbon (Atomergic Chemetals V25) electrode with a platinum foil acting as the counter electrode. Treatment of the electrode surfaces was as reported elsewhere.[9b]

EHMO Calculations. All the calculations were carried out within the standard extended Hückel method[10] with the CAChe program (Version 3.7). Standard atomic parameters were taken for H, C, O, and N.[10b] The exponents (ζ) and the valence shell ionization potential (H_{ii} in eV) used for Re are the standard CAChe parameters,[11] i.e., 2.398 and 9.360 for 6s, 2.372 and 5.960 for 6p, respectively. The H_{ii} value for 5d was 12.660. A linear combination of two Slater-type orbitals (ζ_1 = 5.343, c_1 = 0.6662; ζ_2 = 2.277, c_2 = 0.5910) was used to represent the atomic 5d orbitals.

Crystal Structure Determination. Crystals of **1** were obtained by recrystallization from dichloromethane−*n*-hexane: [C$_{33}$H$_{29}$N$_2$O$_3$Re·0.5((CH$_3$)$_2$O)], fw = 710.85, monoclinic, space group $P2_1/c$ (No. 14), a = 15.574(4) Å, b = 12.634(4) Å, c = 19.030(6) Å, β = 112.19(2)°, V = 3467(1) Å^3, Z = 4, D_c = 1.362 g cm^{-3}, μ(Mo Kα) = 35.39 cm^{-1}, F(000) = 1412, T = 301 K. An orange crystal of dimensions 0.30 × 0.20 × 0.04 mm mounted on a glass fiber was used for data collection at 28 °C on a Rigaku AFC7R diffractometer with graphite-monochromatized Mo Kα radiation (λ = 0.71073 Å) using ω−2θ scans with ω-scan angle (0.68 + 0.35 tan θ)° at a scan speed of 8.0 deg min^{-1} (up to six scans for reflection with $I < 15\sigma(I)$). Intensity data (in the range of $2\theta_{max}$ = 50°; h: 0 to 18; k: 0 to 15; l: −22 to 20 and three standard reflections measured after every 300 reflections showed decay of 0.74%) were corrected for decay and for Lorentz and polarization effects, and empirical absorption corrections were based on the ψ-scan of five strong reflections (minimum and maximum transmission factors 0.516 and 1.000). A total of 6661 reflections were measured, of which 6415 were unique, and R_{int} = 0.048. A total of 3297 reflections with $I > 3\sigma(I)$ were considered observed and used in the structural analysis. The space group was uniquely determined on the basis of systematic absences. The

(7) Eastmond, R.; Walton, D. R. M. *Tetrahedron* **1992**, *28*, 4591−4599.

(8) Perrin, D. D.; Armarego, W. L. F. *Purification of Laboratory Chemicals*, 3rd ed.; Pergamon: Oxford, U.K., 1988.

(9) (a) Gagne, R. R.; Koval, C. A.; Lisensky, G. C. *Inorg. Chem.* **1980**, *19*, 2854. (b) Che, C. M.; Wong, K. Y.; Anson, F. C. *J. Electroanal. Chem., Interfacial Electrochem.* **1987**, *226*, 211.

(10) (a) Hoffmann, R.; Lipscomb, W. N. *J. Chem. Phys.* **1962**, *36*, 2179. (b) Hoffmann, R. *J. Chem. Phys.* **1963**, *39*, 1397.

(11) Dedieu, A.; Albright, T. A.; Hoffmann, R. *J. Am. Chem. Soc.* **1979**, *101*, 3141.

Table 1. Crystal and Structure Determination Data for 1

formula	$[(ReC_{33}H_{29}N_2O_3)\cdot 0.5((CH_3)_2O)]$
fw	710.85
T, K	301
a, Å	15.574(4)
b, Å	12.643(4)
c, Å	19.030(6)
β, deg	112.19(2)
V, Å^3	3467(1)
cryst color	orange
cryst syst	monoclinic
space group	$P2_1/c$ (No. 14)
Z	4
F(000)	1412
D_c, g cm^{-3}	1.362
cryst dimens, mm	0.30 × 0.20 × 0.04
λ, Å (graphite monochromated, Mo Kα)	0.71073
μ, cm^{-1}	35.39
collection range	$2\theta_{max} = 50°$ (h: 0 to 18; k: 0 to 15; l: −22 to 20)
scan mode and scan speed, deg min^{-1}	$\omega-2\theta$, 8.0
scan width, deg	0.68 + 0.35 tan θ
no. of unique data	6415
no. of data used in refinement, m	3297
no. of params refined, p	357
R^a	0.042
wR^a	0.058
goodness-of-fit, S	1.52
maximum shift, $(\Delta/\sigma)_{max}$	0.04
residual extrema in final diff map, e Å^{-3}	+1.21, −0.62

[a] $w = 4F_o^2/\sigma^2(F_o)^2$, where $\sigma^2(F_o)^2 = [\sigma^2(I) + (0.040F_o^2)^2]$ with $I \geq 3\sigma(I)$.

structure was solved by Patterson methods and expanded by Fourier methods (PATTY[12a]), and refinement was by full-matrix least-squares using the software package TeXsan[12b] on a Silicon Graphics Indy computer. One crystallographic asymmetric unit consists of one complex molecule and half of the solvent molecule with O at special position. In the least-squares refinement, all 39 non-H atoms of the complex molecule were refined anisotropically, the O and C atoms of the solvent molecule were refined isotropically, and 29 H atoms at calculated positions with thermal parameters equal to 1.3 times that of the attached C atoms were not refined. H atoms of the solvent molecule were not included. Convergence for 357 variable parameters by least-squares refinement on F with $w = 4F_o^2/\sigma^2(F_o^2)$, where $\sigma^2(F_o^2) = [\sigma^2(I) + (0.040F_o^2)^2]$ for 3297 reflections with $I > 3\sigma(I)$ was reached at $R = 0.042$ and $wR = 0.058$ with a goodness-of-fit of 1.52. $(\Delta/\sigma)_{max} = 0.04$ except for atoms of the solvent molecule. The final difference Fourier map was featureless, with maximum positive and negative peaks of 1.21 and 0.62 e Å^{-3}, respectively. Crystal and structure determination data for **1** are summarized in Table 1. The final agreement factors for **1** are given in Table 1. Selected bond distances and angles are summarized in Table 2. The atomic coordinates and thermal parameters are given as Supporting Information.

Crystals of **3** were obtained by recrystallization from dichloromethane−*n*-hexane: $[C_{24}H_{21}N_2O_3SiRe]$, $M_r = 599.73$, monoclinic, space group $C2/c$ (No. 15), $a = 26.009(2)$ Å, $b = 15.556(2)$ Å, $c = 13.852(2)$ Å, $\beta = 113.484(7)°$, $V = 5140(1)$ Å^3, $Z = 8$, $D_c = 1.550$ g cm^{-3}, μ(Mo Kα) = 48.01 cm^{-1}, F(000) = 2336, $T = 301$ K. A yellow crystal of dimensions 0.20 × 0.20 × 0.05 mm in a glass capillary was used for data collection at 28 °C on a Rigaku AFC7R diffractometer with graphite-monochromatized Mo Kα radiation ($\lambda = 0.71073$ Å) using $\omega-2\theta$ scans with ω-scan angle $(0.63 + 0.35 \tan \theta)°$ at a scan speed of 8.0 deg min^{-1} (up to six scans for reflection with $I < 15\sigma(I)$). Unit-cell dimensions were determined on the basis of the setting angles of 25 reflections in the 2θ range of 36.1−41.5°. Intensity data (in the range of $2\theta_{max} = 50°$; h: 0 to 30; k: 0 to 18; l: −16 to 15 and three standard reflections measured after every 300 reflections showed decay of 0.77%) were corrected for decay and for Lorentz and polarization effects, and empirical absorption corrections based on the ψ-scan of five strong reflections (minimum and maximum transmission factors 0.375 and 1.000). A total of 4821 reflections were measured, of which 4709 were unique and $R_{int} = 0.023$. A total of 3389 reflections with $I > 3\sigma(I)$ were considered observed and used in the structural analysis. The space group was determined on the basis of systematic absences and on a statistical analysis of intensity distribution. The successful refinement of the structure was solved by Patterson methods and expanded by Fourier methods (PATTY[12a]), and refinement was by full-matrix least-squares using the software package TeXsan[12b] on a Silicon Graphics Indy computer. One crystallographic asymmetric unit consists of one molecule. In the least-squares refinement, all 31 non-H atoms were refined anisotropically, and 21 H atoms at calculated positions with thermal parameters equal to 1.3 times that of the attached C atoms were not refined. Convergence for 280 variable parameters by least-squares refinement on F with $w = 4F_o^2/\sigma^2(F_o^2)$, where $\sigma^2(F_o^2) = [\sigma^2(I) + (0.026F_o^2)^2]$ for 3389 reflections with $I > 3\sigma(I)$, was reached at $R = 0.023$ and $wR = 0.029$ with a goodness-of-fit of 1.26. $(\Delta/\sigma)_{max} = 0.03$. The final difference Fourier map was featureless, with maximum positive and negative peaks of 0.56 and 0.57 e Å^{-3}, respectively. Crystal and structure determination data for **3** are summarized in Table 3. The final agreement factors for **3** are given in Table 3. Selected bond distances and angles are summarized in Table 4. The atomic coordinates and thermal parameters are given as Supporting Information.

Table 2. Selected Bond Distances (Å) and Bond Angles (deg) for 1

Re(1)−N(1)	2.179(7)	Re(1)−N(2)	2.175(7)
Re(1)−C(1)	1.95(1)	Re(1)−C(4)	2.120(9)
C(4)−C(5)	1.20(1)	C(6)−C(7)	1.16(1)
C(8)−C(9)	1.18(2)		
N(1)−Re(1)−N(2)	74.7(2)	N(1)−Re(1)−C(2)	172.9(3)
C(1)−Re(1)−C(4)	175.1(3)	C(4)−C(5)−C(6)	177.6(10)
C(5)−C(6)−C(7)	179.0(1)	C(6)−C(7)−C(8)	172.0(1)
C(7)−C(8)−C(9)	175.0(1)		

Results and Discussion

Reaction of a mixture of $[Re(CO)_3(^tBu_2bpy)(C{\equiv}C{-}C{\equiv}CH)]$, $BrC{\equiv}CPh$, piperidine, and CuI in THF at room temperature afforded $[Re(CO)_3(^tBu_2bpy)(C{\equiv}C{-}C{\equiv}C{-}C{\equiv}CPh)]$, **1**, which was isolated as orange crystals after purification by column chromatography on silica gel, followed by recrystallization from dichloromethane−*n*-hexane. On the other hand, reaction of a mixture of $[Re(CO)_3(^tBu_2bpy)(C{\equiv}C{-}C{\equiv}CH)]$, $IC{\equiv}CSiMe_3$, piperidine, and CuI in THF at room temperature afforded $[Re(CO)_3(^tBu_2bpy)(C{\equiv}C{-}C{\equiv}C{-}C{\equiv}CSiMe_3)]$, **2**, which was isolated as orange solid after purification by column chromatography on silica gel, followed by subsequent recrystallization from dichloromethane−*n*-hexane. Similarly, reaction of $[Re(CO)_3(Me_2bpy)(C{\equiv}C{-}C{\equiv}CH)]$, $IC{\equiv}CSiMe_3$, piperidine, and CuI under similar conditions afforded $[Re(CO)_3(Me_2bpy)(C{\equiv}C{-}C{\equiv}C{-}C{\equiv}$

(12) (a) Beurskens, P. T.; Admiraal, G.; Beurskens, G.; Bosman, W. P.; Garcia-Granda, S.; Gould, R. O.; Smits, J. M. M.; Smykalla, C. *The DIRDIF program system*, Technical Report of the Crystallography Laboratory; University of Nijmegen: The Netherlands, 1992. (b) *TeXsan*, Crystal Structure Analysis Package; Molecular Structure Corporation, 1985, 1992.

Table 3. Crystal and Structure Determination Data for 3

formula	$[(ReSiC_{24}H_{21}N_2O_3)$
fw	599.73
T, K	301
a, Å	26.009(2)
b, Å	15.556(2)
c, Å	13.852(2)
β, deg	113.484(7)
V, Å^3	5140(1)
cryst color	yellow
cryst system	monoclinic
space group	$C2/c$ (No.15)
Z	8
F(000)	2336
D_c, g cm^{-3}	1.550
cryst dimens, mm	0.20 × 0.20 × 0.05
λ, Å (graphite monochromated, Mo Kα)	0.71073
μ, cm^{-1}	48.01
collection range	$2\theta_{max} = 50°$ (h: 0 to 30; k: 0 to 18; l: −16 to 15)
scan mode and scan speed, deg min^{-1}	$\omega-2\theta$, 8.0
scan width, deg	0.63 + 0.35 tan θ
no. of unique data	4709
no. of data used in refinement, m	3389
no. of params refined, p	280
R^a	0.023
wR^a	0.029
goodness-of-fit, S	1.26
max shift, $(\Delta/\sigma)_{max}$	0.03
residual extrema in final diff map, e Å^{-3}	+0.56, −0.57

[a] $w = 4F_o^2/\sigma^2(F_o)^2$, where $\sigma^2(F_o)^2 = [\sigma^2(I) + (0.040F_o^2)^2]$ with $I \geq 3\sigma(I)$.

Table 4. Selected Bond Distances (Å) and Bond Angles (deg) for 3

Re(1)−N(1)	2.176(4)	Re(1)−N(2)	2.193(4)
Re(1)−C(1)	1.959(5)	Re(1)−C(4)	2.113(4)
C(4)−C(5)	1.213(6)	C(6)−C(7)	1.195(6)
C(8)−C(9)	1.203(7)		
N(1)−Re(1)−N(2)	74.3(1)	N(1)−Re(1)−C(2)	172.4(2)
C(1)−Re(1)−C(4)	179.8(2)	C(4)−C(5)−C(6)	176.3(5)
C(5)−C(6)−C(7)	178.8(5)	C(6)−C(7)−C(8)	178.7(5)
C(7)−C(8)−C(9)	179.5(6)		

$CSiMe_3$)] (**3**) after purification as orange crystals. The identities of **1**−**3** have been confirmed by satisfactory elemental analyses, ^{1}H NMR spectroscopy, IR, and FAB-MS, and for complexes **1** and **3** also by X-ray crystallography.

Figures 1 and 2 depict the perspective drawings of complexes **1** and **3** with atomic numbering, respectively. Both structures show a slightly distorted octahedral geometry about Re with the three carbonyl ligands arranged in a facial fashion. The N−Re−N bond angles of 74.7(2)° and 74.3(1)° for **1** and **3**, respectively, are less than 90°, as required by the bite distance exerted by the steric demand of the chelating bipyridine ligand. The three C≡C bond lengths are 1.20(1), 1.16(1), and 1.18(2) Å for **1** and 1.213(6), 1.195(6), and 1.203(7) Å for **3**, which are comparable with those found for other related triynyl systems.[5i] The Re−C≡C−C≡C−C≡C unit of **3** is essentially linear, with bond angles of 177.3(4)−179.5(6)°, while that of **1** is slightly bent with bond angles of 173.8(8)−175.0(1)°, which are comparable with those found for a rhenium(I) tolyltriynyl system.[5i]

The electronic absorption spectra of **1**, **2**, and **3** show

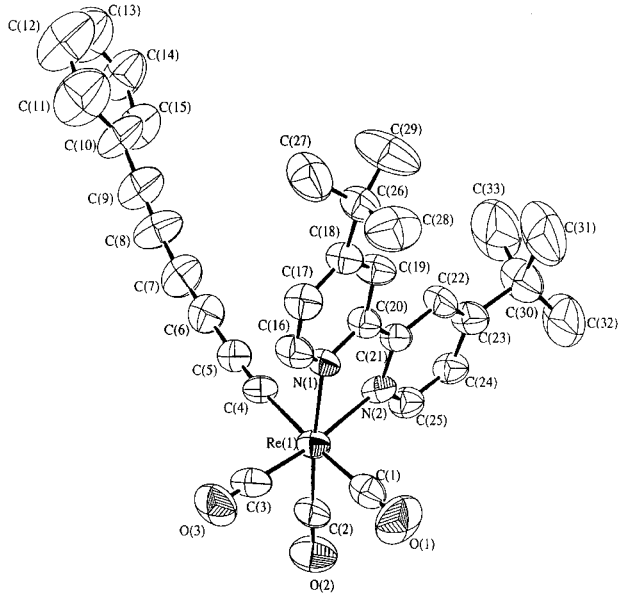

Figure 1. Perspective drawing of complex **1** with atomic numbering. Hydrogen atoms have been omitted for clarity. Thermal ellipsoids were shown at the 40% probability level. Selected bond distances (Å) and bond angles (deg): Re(1)−C(1) 1.95(1), Re(1)−N(1) 2.179(7), Re(1)−N(2) 2.175(7), Re(1)−C(4) 2.120(9), C(4)−C(5) 1.20(1), C(6)−C(7) 1.16(1), C(8)−C(9) 1.18(2), N(1)−Re(1)−N(2) 74.7(2), N(1)−Re(1)−C(2) 172.9(3), C(1)−Re(1)−C(4) 175.1(3), C(4)−C(5)−C(6) 177.6(10), C(5)−C(6)−C(7) 179.0(1), C(6)−C(7)−C(8) 172.0(1), C(7)−C(8)−C(9) 175.0(1).

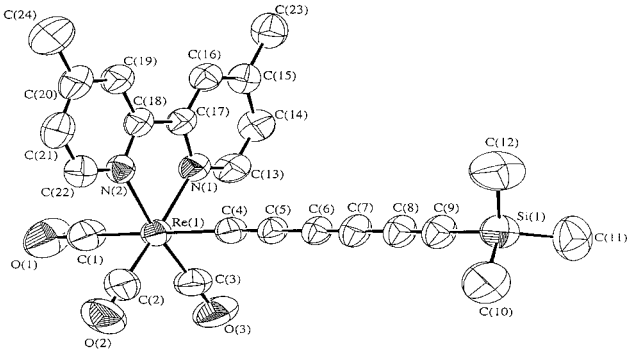

Figure 2. Perspective drawing of complex **3** with atomic numbering. Hydrogen atoms have been omitted for clarity. Thermal ellipsoids were shown at the 40% probability level. Selected bond distances (Å) and bond angles (deg): Re(1)−C(1) 1.959(5), Re(1)−N(1) 2.176(4), Re(1)−N(2) 2.193(4), Re(1)−C(4) 2.113(4), C(4)−C(5) 1.213(6), C(6)−C(7) 1.195(6), C(8)−C(9) 1.203(7), N(1)−Re(1)−N(2) 74.3(1), N(1)−Re(1)−C(2) 172.4(2), C(1)−Re(1)−C(4) 179.8(2), C(4)−C(5)−C(6) 176.3(5), C(5)−C(6)−C(7) 178.8(5), C(6)−C(7)−C(8) 178.7(5), C(7)−C(8)−C(9) 179.5(6).

intense absorption bands at ca. 426, 412, and 420 nm, respectively, in tetrahydrofuran. With reference to previous spectroscopic work on rhenium(I) diimine systems,[3a,b,f−h,13] the intense low-energy absorption is tentatively assigned as the dπ(Re) → π^*(^{t}Bu$_2$bpy or Me$_2$bpy) MLCT transition. The lower MLCT absorption energy for **1** than **2** is consistent with the better

(13) (a) Wrighton, M. S.; Morse, D. L. *J. Am. Chem. Soc.* **1974**, *96*, 998. (b) Wrighton, M. S.; Morse, D. L.; Pdungsap, L. *J. Am. Chem. Soc.* **1975**, *97*, 2073. (c) Tapolsky, G.; Duesing, R.; Meyer, T. J. *Inorg. Chem.* **1990**, *29*, 2285. (d) Hino, J. K.; Ciana, L. D.; Dressick, W. J.; Sullivan, B. P. *Inorg. Chem.* **1992**, *31*, 1072.

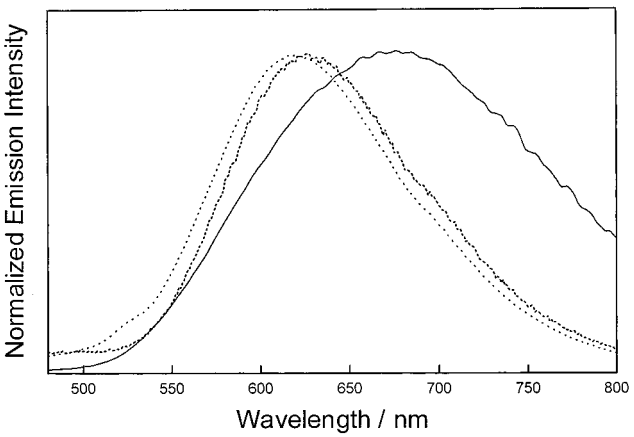

Figure 3. Normalized emission spectra of $Re(CO)_3(^tBu_2bpy)(C{\equiv}CPh)$ (—), $Re(CO)_3(^tBu_2bpy)(C{\equiv}CC{\equiv}CPh)$ (- - -), and $Re(CO)_3(^tBu_2bpy)(C{\equiv}CC{\equiv}CC{\equiv}CPh)$ (···) in degassed THF at 298 K.

π-donating abilities of $PhC{\equiv}C{-}C{\equiv}C{-}C{\equiv}C$ than $Me_3SiC{\equiv}C{-}C{\equiv}C{-}C{\equiv}C$, which render the Re(I) center more electron rich and raise the Re dπ orbital energy. An alternative assignment of a $\pi(RC{\equiv}C{-}C{\equiv}C{-}C{\equiv}C)$ to $\pi^*(^tBu_2bpy$ or $Me_2bpy)$ ligand-to-ligand charge transfer (LLCT) transition is also possible and cannot be completely excluded. Similar trends have been observed in the related alkynyl system $[Re(CO)_3(^tBu_2bpy)X]$,[3a] in which the MLCT absorption band occurs at higher energy for $X = Me_3SiC{\equiv}C$ than when $X = PhC{\equiv}C$.

Excitation of **1**−**3** both in the solid state and in fluid solutions at room temperature at $\lambda > 400$ nm resulted in strong orange luminescence, attributed to the ^{3}MLCT phosphorescence. The lower MLCT emission energy of **1** than **2** in THF is in line with the stronger π-donating abilities of the phenyltriynyl unit than the trimethylsilyltriynyl ligand, i.e., $PhC{\equiv}C{-}C{\equiv}C{-}C{\equiv}C$ (620 nm) < $Me_3SiC{\equiv}C{-}C{\equiv}C{-}C{\equiv}C$ (596 nm). Similar trends have been observed in the monoacetylide analogues [$PhC{\equiv}C$ (688 nm) < $Me_3SiC{\equiv}C$ (670 nm)].[3a] It is interesting to note that both **1** and **2** emit at higher energies than their respective monoynyl and diynyl counterparts; that is, in the $[Re(CO)_3(^tBu_2bpy)X]$ system, the emission energies in THF follow the order $PhC{\equiv}C{-}C{\equiv}C{-}C{\equiv}C$ (620 nm) > $PhC{\equiv}C{-}C{\equiv}C$ (625 nm) > $PhC{\equiv}C$ (688 nm); $Me_3SiC{\equiv}C{-}C{\equiv}C{-}C{\equiv}C$ (596 nm) > $Me_3SiC{\equiv}C$ (670 nm). Figure 3 shows the emission spectral trend of the complexes as a function of the acetylenic carbon chain length. The observation of a blue shift in emission energies upon increasing the C≡C unit disfavors an assignment of a ^{3}MLCT [dπ(Re) → $\pi^*((C{\equiv}C)_nR)$] or a metal-perturbed ^{3}IL [$\pi((C{\equiv}C)_nR) \rightarrow \pi^*((C{\equiv}C)_nR)$] origin ($n = 1, 2, 3$) and may be more suggestive of an assignment of a ^{3}MLCT [dπ(Re) → $\pi^*(^tBu_2bpy)$] or ^{3}LLCT [$\pi((C{\equiv}C)_nR) \rightarrow \pi^*(^tBu_2bpy)$] origin. Molecular orbital studies using extended Hückel molecular orbital (EHMO) theory on **1** and its diynyl analogue $[Re(CO)_3(^tBu_2bpy)(C{\equiv}C{-}C{\equiv}CPh)]$ show that in both the diynyl and triynyl systems the LUMO mainly consists of $\pi^*(^tBu_2bpy)$ character, while the HOMO is mainly dominated by the antibonding character of the $Re{-}(C{\equiv}C)_nPh$ ($n = 2, 3$) moiety resulting from the overlap of the dπ(Re) and $\pi[(C{\equiv}C)_nPh]$ orbitals, which is supportive of a mixed dπ(Re) → $\pi^*(^tBu_2bpy)$ MLCT/$\pi((C{\equiv}C)_nR) \rightarrow \pi^*(^tBu_2bpy)$ LLCT character for the electronic transition. Table 6 summarizes the calculated molecular orbital energies, percentage composition, and the HOMO−LUMO energy gap. An increase in the HOMO−LUMO energy gap has been observed on extending the C≡C unit from the diynyl (calc $\Delta E_{gap} = 2.40$ eV) to the triynyl species (calc $\Delta E_{gap} = 2.59$ eV), in which the LUMO energies remain more or less the same while the HOMO energies decrease with an increasing number of C≡C units. The observed trend of a higher MLCT/LLCT emission energy in the triynyl system than the diynyl and hence the monoynyl systems, in line with EHMO studies, may originate from a decreased overlap integral between the dπ(Re) and the triynyl $\pi(RC{\equiv}CC{\equiv}CC{\equiv}C)$ orbitals than that of dπ(Re) and the $\pi(RC{\equiv}CC{\equiv}C)$ and $\pi(RC{\equiv}C)$ orbitals resulting from the delocalization of electron density across the C_n unit, despite the better energy match between $\pi(RC{\equiv}CC{\equiv}CC{\equiv}C)$ and the dπ(Re) orbital. In other words, the overlap of the closely energy matched dπ(Re) and $\pi(RC{\equiv}CC{\equiv}CC{\equiv}C)$ orbitals does not necessarily raise the HOMO to an energy higher than that for the diynyl and monoynyl cases and may give rise to the anomalous energy trend in which the MLCT/LLCT emission energy is in the order $PhC{\equiv}C{-}C{\equiv}C{-}C{\equiv}C > PhC{\equiv}C{-}C{\equiv}C > PhC{\equiv}C$. An alternative rationale for the increased MLCT energies upon increasing the C≡C units is that given the similar σ-donating properties of the monoynyl, diynyl, and triynyl unit,[1a,14] the much better π-accepting ability of $RC{\equiv}C{-}C{\equiv}C{-}C{\equiv}C$ than $RC{\equiv}C{-}C{\equiv}C$, which in turn is better than $RC{\equiv}C$, may become the dominating factor, stabilizing the Re dπ orbitals to a greater extent, and hence gives rise to a higher energy ^{3}MLCT [dπ(Re) → $\pi^*(^tBu_2bpy$ or $Me_2bpy)$] emission. However, in view of the much lesser importance of the $d\pi(Re){-}\pi^*[(C{\equiv}C)_nR]$ interaction, as reflected from EHMO studies, such possibilities are less likely.

The cyclic voltammograms of complexes **1**−**3** in acetonitrile (0.1 mol dm^{-3} $^nBu_4NPF_6$) display an irreversible oxidation wave (+1.12 to +1.17 V vs SCE) and one quasi-reversible oxidation couple (+1.77 to +1.81 V vs SCE), while one quasi-reversible reduction couple (−1.46 to −1.47 V vs SCE) is observed in the reductive scan. The electrochemical data are summarized in Table 7. The reduction couple was tentatively assigned as a bipyridyl ligand-centered reduction,[15] as it occurred at almost identical potential for complexes **1**−**3**, where the electron-donating effect of the methyl groups and *tert*-butyl groups on the bipyridine ligands are similar. The first oxidation wave, which occurred at ca. +1.10 V vs SCE, was tentatively assigned as a Re(I) to Re(II) oxidation process. The observation that complex **1** shows a less positive potential for its oxidation wave than that of complex **2** is consistent with the better π-donating abilities of the phenyltriynyl unit than the trimethylsilyltriynyl ligand, which would render the rhenium(I) metal center more electron rich and hence increases its ease of oxidation. Such an increased ease of metal-

(14) (a) Lichtenberger, D. L.; Renshaw, S. K. *Organometallics* **1993**, *12*, 3522. (b) Lichtenberger, D. L.; Renshaw, S. K.; Bullock, R. M. *J. Am. Chem. Soc.* **1993**, *115*, 3276.

(15) (a) Smothers, W. K.; Wrighton, M. S. *J. Am. Chem. Soc.* **1983**, *105*, 1067. (b) Hawecker, J.; Lehn, J. M.; Ziessel, R. *Helv. Chim. Acta* **1986**, *69*, 1990. (c) Vogler, A.; Kunkel, H. *Inorg. Chem.* **1987**, *26*, 1819. (d) Wallace, L.; Woods, C.; Rillema, D. P. *Inorg. Chem.* **1995**, *34*, 2875. (e) Yam, V. W. W.; Lau, V. C. Y.; Cheung, K. K. *Organometallics* **1995**, *14*, 2749. (f) Yam, V. W. W.; Lau, V. C. Y.; Cheung, K. K. *Organometallics* **1996**, *15*, 1740.

Table 5. Photophysical Data for Complexes 1−3

complex	medium (T/K)	emission λ_{em}/nm (τ_o/μs)	absorption λ_{max}/nm (ϵ/dm^3 mol^{-1} cm^{-1})
1	THF (298)	620 (<0.05)	254 (52580), 300 sh (61680), 426 (3810)
	solid (298)	585 (<0.05)	
	solid (77)	590	
	EtOH−MeOH glass (4:1 v/v) (77)	528, 596	
2	THF (298)	596 (0.1)	250 (3940), 296 (3290), 350 sh (4370), 412 (2160)
	solid (298)	585 (<0.05)	
	solid (77)	575	
	EtOH−MeOH glass (4:1 v/v) (77)	496, 556	
3	THF (298)	615 (<0.05)	248 (33140), 298 sh (2740), 420 (3790)
	solid (298)	580 (0.14)	
	solid (77)	580	
	EtOH−MeOH glass (4:1 v/v) (77)	497, 557	

Table 6. Calculated Molecular Orbital Energies and Transition Energies

complex	no.	level/eV	composition/%				HOMO−LUMO energy gap, ΔE_{gap}/eV
			Re	(C≡C)$_n$Ph	3CO	^{t}Bu$_2$bpy	
1	101	−8.9570	5	25	64	4	2.5922 (98 → 99)
	100	−9.0440	*a*	89	8	*a*	
	99 (LUMO)	−9.5499	*a*	*a*	2	91	
	98 (HOMO)	−12.1421	9	77	4	*a*	
	97	−12.1611	12	74	6	*a*	
	96	−12.2699	4	4	*a*	85	
[Re(CO)$_3$(^{t}Bu$_2$bpy)(C≡C−C≡CPh)]	97	−8.8400	2	5	18	69	2.4018 (94 → 95)
	96	−9.0277	1	75	18	1	
	95 (LUMO)	−9.5907	*a*	*a*	*a*	91	
	94 (HOMO)	−11.9925	12	78	6	*a*	
	93	−12.2373	16	58	4	13	
	92	−12.3080	5	8	2	81	

[a] Percentage composition of less than 0.5%.

Table 7. Electrochemical Data for Complexes 1−3[a]

complexes	$E_{1/2}$[b]/V vs SCE (ΔE_p/mV)	
	reduction[c]	oxidation[c]
1	−1.46 (76)	+1.12
		+1.80 (60)
2	−1.46 (69)	+1.17
		+1.77 (72)
3	−1.47 (81)	+1.16
		+1.81 (55)

[a] In acetonitrile (0.1 mol dm^{-3} ^{n}Bu$_4$NPF$_6$). Working electrode: glassy carbon; ΔE_p of Fc$^+$/Fc ranges from 62 to 64 mV. [b] $E_{1/2} = (E_{pa} + E_{pc})/2$; E_{pa} and E_{pc} are peak anodic and peak cathodic potentials, respectively. [c] Scan rate, 100 mV s^{-1}.

centered oxidation for complex **1** than **2** is also in accord with the lower absorption and emission energies observed in **1** than **2** and further supports their assignments as transitions of mixed MLCT/LLCT nature. The second oxidation wave, which occurred at ca. +1.80 V vs SCE, was found to be relatively insensitive to the nature of the acetylide ligand. As the potential values of the second oxidation for the rhenium(I) acetylide complexes are similar and comparable to the corresponding analogues, [Re(CO)$_3$(^{t}Bu$_2$bpy)(MeCN)]$^+$ and [Re(CO)$_3$(Me$_2$bpy)(MeCN)]$^+$ in acetonitrile,[16] an EC mechanism was proposed for the oxidation of the complexes. In the proposed EC mechanism, a weakening of the bonding between the metal center and the acetylide ligand occurred after the first oxidation, which resulted in the loss of an acetylide radical to give the coordinatively unsaturated intermediates [Re(CO)$_3$(^{t}Bu$_2$bpy)]$^+$ and [Re(CO)$_3$(Me$_2$bpy)]$^+$, which then readily picked up an acetonitrile molecule from the solvent to form the corresponding [Re(CO)$_3$(^{t}Bu$_2$bpy)(MeCN)]$^+$ and [Re(CO)$_3$(Me$_2$bpy)(MeCN)]$^+$, respectively. Therefore the second oxidation process was tentatively assigned as the oxidation of Re(I) to Re(II) of [Re(CO)$_3$(^{t}Bu$_2$bpy)(MeCN)]$^+$ and [Re(CO)$_3$(Me$_2$bpy)(MeCN)]$^+$. The observation that complexes **1**−**3** show similar positive potential for their second oxidation waves is consistent with the similar electron-donation effect of the methyl groups and *tert*-butyl groups.

Conclusion

Several luminescent rhenium(I) triynyl complexes of substituted 2,2′-bipyridines were successfully synthesized. The blue shift in emission energy upon extending the carbon chain in these complexes represents an unusual phenomenon contradictory to the common concept of tuning the emission energy to the red by extending the number of acetylenic units in organic polyynes. This demonstrates the importance and versatility of systematic structural variation in elucidating the spectroscopic origins of these systems and the flexibility of emission energies' tuning simply by changing the nature of the excited state origin.

Acknowledgment. V.W.-W.Y. acknowledges financial support from the Research Grants Council and The University of Hong Kong, and S.H.-F.C. and C.-C.K. acknowledge the receipt of a postgraduate studentship, administered by The University of Hong Kong. Helpful and insightful discussions with Professor J.-F. Halet are gratefully acknowledged. The award of a grant by the CNRS/RGC under the PROCORE France-Hong Kong Joint Research Scheme is gratefully acknowledged.

Supporting Information Available: Tables giving fractional coordinates and thermal parameter expressions (U) and all bond distances and bond angles. This material is available free of charge via the Internet at http://pubs.acs.org.

OM000725B

(16) (a) Breikss, A. I.; Abruna, H. D. *J. Electroanal. Chem.* **1986**, *201*, 347. (b) Lau, V. C. Y. Ph.D. Thesis, The University of Hong Kong, 1997.